We are IntechOpen, the world's leading publisher of Open Access books Built by scientists, for scientists

4,800
Open access books available

122,000
International authors and editors

135M
Downloads

Our authors are among the

154
Countries delivered to

TOP 1%
most cited scientists

12.2%
Contributors from top 500 universities

CLARIVATE ANALYTICS BOOK CITATION INDEX INDEXED

WEB OF SCIENCE™

Selection of our books indexed in the Book Citation Index in Web of Science™ Core Collection (BKCI)

Interested in publishing with us?
Contact book.department@intechopen.com

Numbers displayed above are based on latest data collected.
For more information visit www.intechopen.com

19

Soft Lithographic Fabrication of Micro Optic and Guided Wave Devices

Angel Flores and Michael R. Wang
University of Miami
U.S.A.

1. Introduction

Since the advent of the laser, guided wave and integrated optical devices have attracted significant research interest for use in advanced telecommunication and interconnection systems. Based on the device substrate or material used, i.e., silicon, LiNaO, LiTaO, GaAs, or polymer, different manufacturing techniques have been developed for fabrication of these optical devices. While various methods can effectively produce guided wave devices, none have been able to match the high-yield, low-cost, mass productivity schemes that define the photolithographic technique in the semiconductor industry.

For example, silicon and silicon dioxide waveguides (Bowers, et al., 2007) are normally produced through standard photolithographic methods; requiring customary thin film deposition (sputtering, chemical vapor deposition, or thermal oxidation), UV mask exposure, and post dry-etching procedures. Despite their high yields and exceptional cost performance, photolithography demands the use of a clean-room facility equipped with elaborate semiconductor manufacturing equipment (sputtering machine, e-beam evaporator, mask aligner, reactive-ion etcher, to name a few), leading to undesirable startup costs and prolonged lead times. Similarly, advanced manufacturing schemes derived from semiconductor production methods, including epitaxial growth waveguides (Brown, et al., 1987) experience comparable cost-prohibitive drawbacks.

Waveguides fabricated on glass substrates typically rely on an ion-exchange process (Ramaswamy & Srivastava, 1988) that may circumvent some of the equipment overhead required in photolithography. In the ion exchange process, the device substrate is placed in a molten cation bath causing the sodium ions in the glass substrate to exchange with one of the cations (ie., K^+, Li^+, Cs^+). The ion alteration raises the local refractive index of the substrate and creates a waveguiding region in the glass. Because of their low propagation losses, minimal production costs, and compatibility with optical fibers, the use of ion-exchange waveguides for integrated optical applications has been extensively researched. In spite of its advantages, issues regarding device yield and reproducibility still remain.

Consequently, polymers have become an attractive alternative to glass and Si/SiO_2 as materials for optical waveguide devices. Polymers are less fragile and less expensive than glass and silicon. Fittingly, polymer waveguides can be made flexible, accommodating non-planar approaches. On the other hand, waveguides fabricated on glass or semiconductor substrates are normally nonflexible and limited to static planar applications. Furthermore, fabrication of polymer devices is aided through mass-replication techniques. The fabrication

Source: Lithography, Book edited by: Michael Wang,
ISBN 978-953-307-064-3, pp. 656, February 2010, INTECH, Croatia, downloaded from SCIYO.COM

methods generally used to create polymer devices are based on casting, embossing, or injection molding (Heckele & Schomburg, 2004) replication techniques that are normally faster and more cost effective than conventional photolithographic and ion exchange methods used on glass and Si/SiO_2 materials. More recently, soft-molding replication techniques known as soft lithography are being actively investigated for low-cost, rapid micro-device replication. To that end, we have been researching diverse soft lithographic techniques for guided wave device fabrication.

Soft lithography is a micro-fabrication technique that has been shown to generate high quality micro and nanostructures as small as 10 nm. It eliminates the use of costly and time-consuming lithographic techniques and equipment. Unlike photolithography which is expensive, has little flexibility in material selection, cannot be applied to non-planar surfaces, and provides little control over chemistry of patterned surfaces; soft lithography can circumvent many of these problems. Soft lithography can tolerate a wide selection of materials, can be used for non-planar and three-dimensional structure fabrication, and most importantly can reproduce high-resolution nano/microstructures at very low cost. As a result, soft lithography has generated considerable research interest over the past decade.

Similarly, microfluidic systems with a broad range of chemical and biological applications continue to be an active research area. Microfluidic based devices process or control small amounts of fluids through utilization of channels with micrometer dimensions (Whitesides, 2006). Particularly, a few of the widely reported microfluidic applications include forensics, gene expression assays (Liu et al., 1999), environmental tests (van der Berg et al., 1993), biomedical implantable devices (Santini et al., 1998), and clinical blood analysis (Lauks, 1998). To date, the majority of microfluidic systems have been fabricated using either photolithography, hard replica molding, or more recently, soft lithographic methods (Xia & Whitesides, 1998). Correspondingly, in this chapter we introduce and describe a novel soft lithographic fabrication technique; a vacuum assisted microfluidic (VAM) method that eliminates the polymer background residue inherent in traditional soft molding fabrication techniques. Incorporation of a microfluidic approach with soft lithography allows high-quality guided wave devices to be fabricated rapidly and inexpensively.

The VAM technique is used to develop guided wave devices including single mode and multimode channel waveguides, and array waveguide evanescent coupler (AWEC) ribbons for high speed optical interconnections. The fabrication of these devices demonstrates the cost effectiveness and promise of the proposed approach for the development of inexpensive, high-quality, and mass-produced polymer guided wave devices.

2. Soft lithography

Soft lithography represents a set of high-resolution patterning techniques in which an elastomeric stamp or mold is used for pattern definition. Once the replica stamp is created, multiple copies of the pattern can be defined through straightforward experimental methods. These non-lithographic techniques require minimal monetary investment (clean room not necessary), can be conducted under normal bench top laboratory conditions, and are conceptually simple to fabricate. Some of the diverse fabrication methods known collectively as soft lithography include: replica molding (Xia et al., 1997), micromolding in capillaries-MIMIC (Zhang et al., 2002), microcontact printing-μCP (Quist et al., 2005), and microtransfer molding-μTM (Zhao et al., 1996). Schematic illustrations of some these procedures are depicted in Fig. 1.

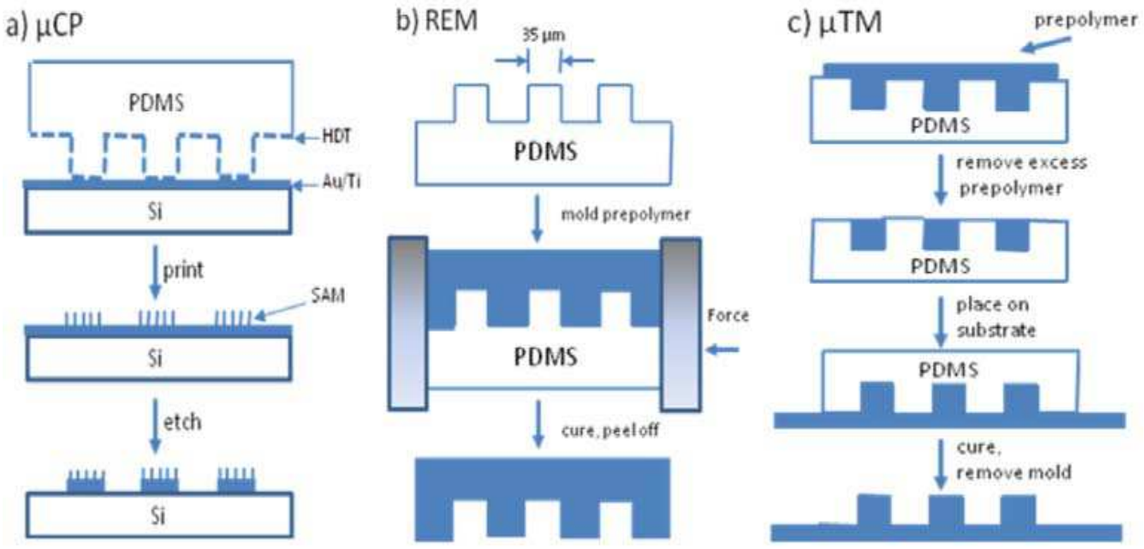

Fig. 1. Schematic illustrations of soft lithographic techniques for a) microcontact printing (μCP), b) replica molding (REM), and c) microtransfer molding (μTM).

Microcontact printing is a flexible, non-photolithographic method that forms patterned self assembled monolayers (SAM) with micron to nanometer scale dimensions. SAMs are surfaces consisting of a single layer of molecules which are prepared by adding a solution of the molecule to the substrate and washing off the excess mixture. Depending on the molecular structure and substrate surface, various molecules can be self assembled without the use of molecular beam epitaxy or vapor deposition. The procedure, demonstrated in Fig. 1a, is simple; an elastomeric polydimethylsiloxane (PDMS) stamp is used to transfer molecules of a hexadecanethiol (HDT) ink to the gold surface of the substrate by contact. After printing, any undesired gold material can be etched away to yield the desired pattern. The technique has been shown to be successful for device fabrication on non-planar surfaces and complex micro patterns.

In replica molding (REM), shown in Fig. 1b, an elastomeric mold rather than a rigid mold, is used to create replica patterns (Xia et al., 1997). Here the organic polymer is placed in contact with the PDMS while the mold is being deformed or compressed in a controlled manner. Deformation of the elastomer provides a method to fabricate structures that would be difficult or unpractical through other procedures.

Alike in several ways, μTM is based on the application of a liquid prepolymer against a patterned PDMS mold. After the excess liquid is removed (by scraping or blowing), the filled mold is placed in contact with a substrate, cured and then peeled to generate the patterned microstructure. Subsequently, soft lithography represents a collection of quick and convenient replication techniques suitable for the definition of both large core (> 100 μm) and nanometer scale devices as well as nanostructures. Through utilization of soft lithographic methods several optical and photonic components have already been successfully demonstrated, such as photonic bandgap structures (Schueller, et al., 1999), distributed feedback structures (Rogers et al., 1998), and microlens arrays (Kunnavakkam et al., 2003). Notably, the lower cost, ease of fabrication, rapid prototyping, and high resolution patterning capabilities are well suited for the replication of guided wave devices.

2.1 Master and PDMS stamp fabrication

The key elements in soft lithography are transparent elastomeric PDMS stamps with patterned relief structures on its surface. PDMS is a polymer having the elastic properties of natural rubber that is able to deform under the influence of force and regain its shape when the force is released. This enables PDMS to conform to substrate surfaces over a large area and adapt to form complex patterned structures. Accordingly, our PDMS molds are produced with Sylgard 184 from Dow Corning; a two-part elastomer that is commercially available at low cost. Once a replica stamp is created, multiple copies of the pattern can be defined through straightforward experimental methods, as illustrated in Fig. 1.

A schematic illustration of the PDMS stamp fabrication process is depicted in Fig. 2. A master silicon device (channel waveguide array) is developed in SU-8 photoresist through photolithography, as shown in Fig. 2a. To begin, SU-8 is spin coated and exposed to UV irradiation through a chromium photomask using a mask aligner. The mask, created via laser-direct writing (Wang & Su, 1998), is a positive replica of the desired channel waveguide arrays. After post exposure baking and photoresist development, the waveguide array master device is realized. Notably, SU-8 patterns processed on silicon wafers are robust, durable and can be used indefinitely (Saleh & Sohn, 2003).

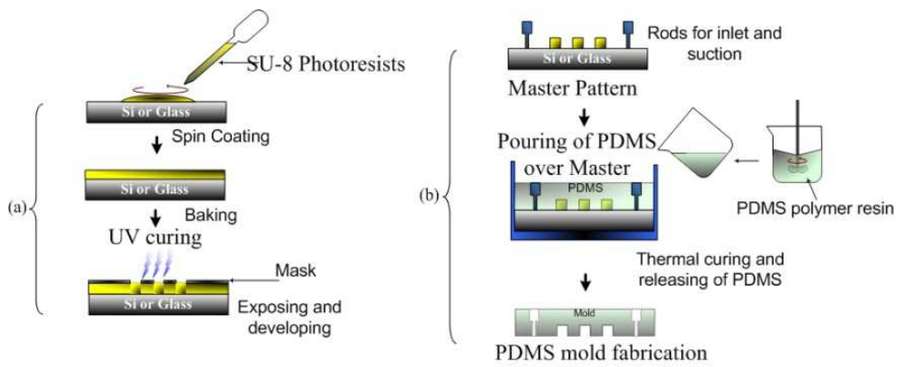

Fig. 2. a) Master pattern development process using SU-8 photoresist. (b) Subsequent generation of the PDMS replication stamp.

Once the master pattern is formed, casting the PDMS prepolymer against the desired surface profile generates a negative replica stamp. The prepolymer is left to settle for 8 hours to eliminate bubbles (and uniformly settle) and then baked for 1h at 60ºC. After thermal curing, the solid prepolymer was peeled off to produce a PDMS replica stamp, as shown in Fig. 2b. The replica stamps can be used to create high-fidelity (nanometer scale) copies of the original master pattern. Additionally, the stamps can be reused multiple times (50~100 times) without degradation for mass replication. Such favorable traits have led to the exploration of soft lithography for low cost, mass prototyping device fabrication.

2.2 Microtransfer molding (μTM)

Subsequently, initial fabrication of our guided wave devices was based on microtransfer molding. μTM relies on conformal contact between the stamp and substrate surface to create the waveguide patterns. The approach represents the simplest and most cost-effective fabrication strategy. A schematic description of a standard μTM approach for polymeric waveguide fabrication is presented in Fig. 3a. To begin, the device substrate is coated with a low index buffer to act as the cladding layer. Then, a UV curable prepolymer resin is applied

onto the PDMS stamp and placed in direct contact with the device substrate. Next, adequate force is uniformly applied to the stamp to assist in the pattern generation. Consequently, UV irradiation through the transparent PDMS mold creates a crosslinking reaction to solidify the waveguide core pattern. After the resin is cured to a solid, the mold is lifted-off (peeled) to leave a patterned structure on the substrate.

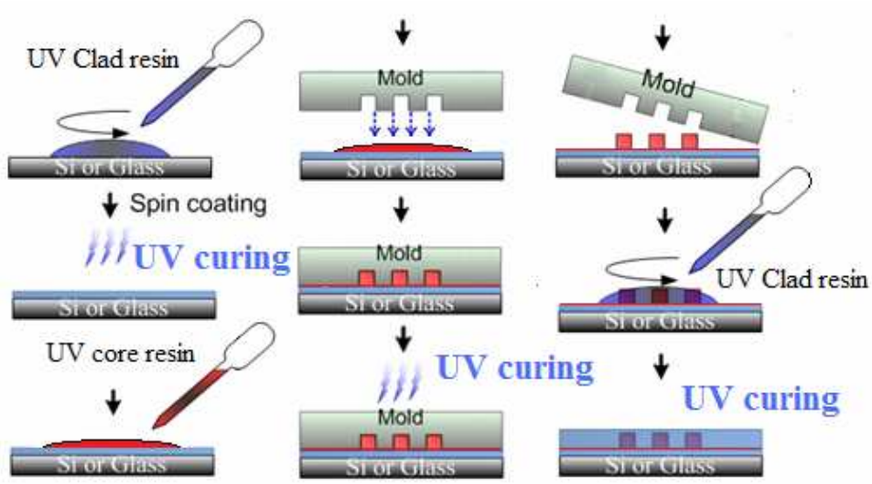

(a)

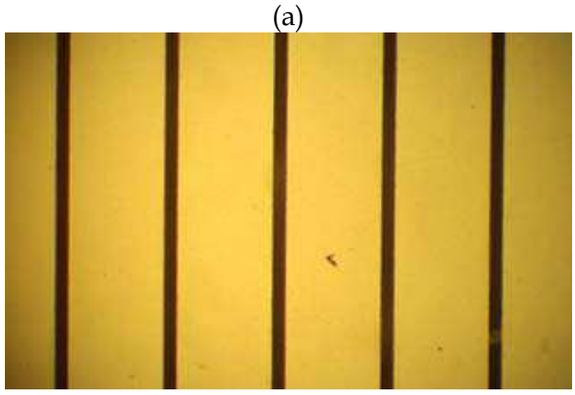

(b)

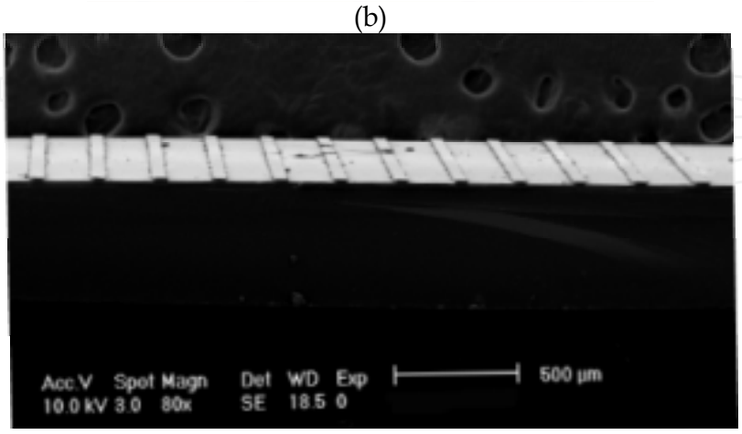

(c)

Fig. 3. Schematic illustration of polymeric waveguide fabrication via µTM (a). Micrographs (20× objective) of 35 µm wide master waveguide array (b) and replicated waveguide array (c).

Microscopic images of the master and replicated channel waveguide arrays are shown in Figs. 3b and 3c. Significantly, surface profile measurements exhibit near identical dimensions. We note that because the PDMS mold acts as a secondary master with no influence on the master fabrication, as long as a lower index cladding (or buffer) layer is processed on top of the substrate, a wide array of substrate materials such as glass, silicon wafer, or polymers can be employed. This will be advantageous as we begin to explore lithe substrates for flexible waveguide performance.

Microtransfer molding can generate microstructures over relatively large areas within a short period of time (<1 min). In addition, once the stamp is developed it can be reused many times for device replication. Due to its quick curing time and substantial working area the microtransfer molding technique can be used for fast and accurate prototyping. Nevertheless, it is important to mention that the elasticity of PDMS also leads to several drawbacks. For example, aspect ratios that are too high or too low cause the microstructures in PDMS to deform or distort. Gravity, adhesion and capillary forces exert stress on the elastomeric material causing it to collapse and generate defects in the pattern. Some of the common defects affecting PDMS generation including feature sagging, ineadequate aspect ratios and surface nonuniformity are a consequence of force applied during the soft molding pattern generation. Solutions to these and other common defects affecting PDMS replication including polymer residue and structure warping will be explored later.

3. Polymeric waveguide

The polymer material design is critical for the desired high-performance, high-resolution and low-loss guided wave device. As such, novel UV curable polymeric waveguide materials were developed (Song, S., et al., 2005). The waveguide materials are specifically suited for the fabrication of guided wave devices using soft lithography. The material adheres to the device substrate upon curing without bonding to the PDMS mold during lift-off (peel). Furthermore, we anticipate using both single mode and multimode waveguide structures so the material should be able to create small and large-core devices.

We designed and synthesized two types of photo curable oligomers; epoxy and acrylate oligomers. The epoxy type oligomer resins were prepared from commercially available dihydroxy (OH) monomers and epichlorohydrin. The acrylate oligomers were synthesized in two steps consisting of an initial reaction between the polyol and diisocyanate monomers, followed by the reaction between the first step byproduct and hydroxy-terminated methacrylate monomers. Their respective chemical schemes are shown in Figure 4.

Ultimately, the epoxy type resins outperformed the acrylate oligomers in terms of UV curing time, with the epoxy resins curing in about 30 seconds under 20,000 mW/cm^2 UV irradiation. The prepolymer resins were formulated from the synthetic oligomer, diverse photo curable monomers, additives, and catalytic amounts of photoinitiators. After all the reagents were discharged in a bottle they were dispersed and mixed in an ultrasonic bath for 15~30 min. The formulation study focused on reducing the curing time, shrinkage and determining the proper viscosity. The curing reactivity and viscosity of the resin can be controlled by addition of multifunctional monomers. The general formulation ratio utilized is given below:

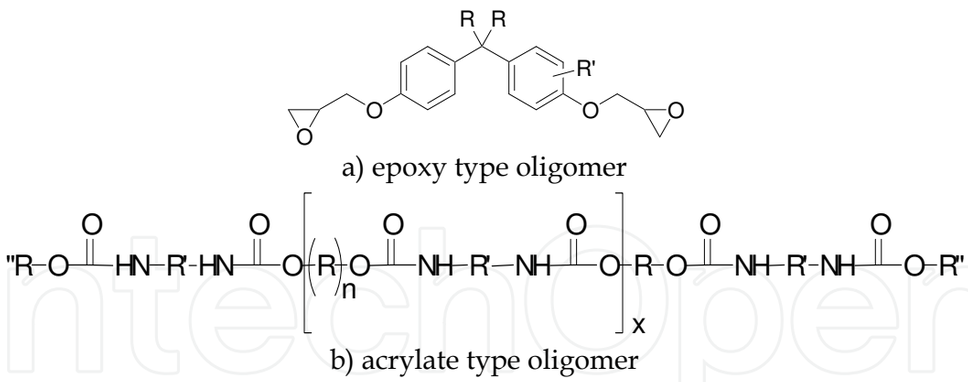

Fig. 4. Chemical structures of the UV curable oligomers for polymeric waveguides. a) The substituent R and R′ represent the fluorinated or non-fluorinated chemical groups, and b) the terminal substituent R″ is the acrylate group.

Fluorinated oligomers: 10 ~ 50%
Multifunctional monomers: 20 ~ 60%
Monofunctional additives: 5 ~ 20%
Photoinitiator: 1 ~ 5%
Other additives: 1 ~ 5 %

The roll of the fluorinated oligomer is an integral part of the composite resin and is very important for determining waveguide properties such as refractive index, optical loss, and hardness of the cured solid. Resins for both the core (CO-1) and cladding (C1-1) waveguide materials were synthesized, where the core material was designed with a marginally higher refractive index.

After synthesizing the waveguide material we analyzed some of its optical properties. The spectrum of both CO-1 and C1-1 (15 micron thick film samples) were measured with a UV-VIS-NIR spectrophotometer. The plot, shown in Fig. 5, discloses the excellent optical transparencies (> 90%) of the synthesized materials in the visible to near IR communication region. Significantly, the flat transparency curve allows for future flexibility in wavelength

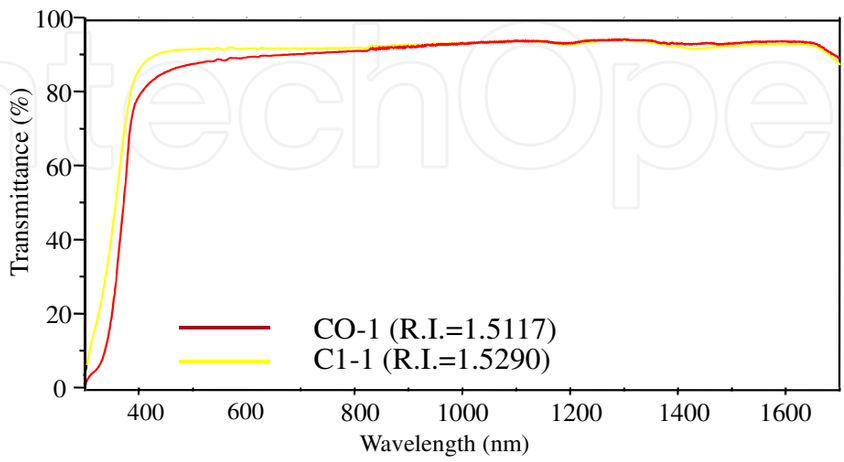

Fig. 5. Transmittance spectrum of formulated core and cladding material measured with a UV-VIS-NIR spectrophotometer.

selection. After establishing excellent optical transparency, the refractive indices of the core and cladding materials were carefully regulated. The refractive index can be explicitly controlled through alteration of the formulation ratio in the fluorinated oligomer portion. Specifically, the final waveguide core and cladding resins exhibited refractive indices of 1.5117 and 1.5290, respectively (Δn = 0.011).

In conclusion, polymeric waveguide resins based on fluorinated oligomers were developed. The material developed consists of a controlled mixture of fluorinated epoxy type oligomers, various photo curable additives, and photoinitiators. The polymer material exhibits excellent broadband (visible to near IR) optical transparency, tunable index control, rapid curing, and light guiding functionality. Moreover, the materials were specifically tailored to meet our soft lithographic fabrication technique which enables rapid device prototyping.

Array waveguide device replication

Once the prepolymer resins were developed, the feasibility of the proposed approach for guided wave device replication was assessed through production of 12 channel waveguide arrays using μTM. BeamPROP software from Rsoft Inc. was employed to design the waveguide array depicted in Fig. 6a. Accordingly, the electric field distribution of the AWEC device is shown on the right. The 12-channel waveguide array (each 10 mm long) has dimensions of 35 μm by 35 μm with a 250-micron pitch. Notably, the 250-micron pitch represents the standard pitch for optical transmitter/receiver arrays. A cross section schematic of the waveguide array device is also presented in Fig. 6b, where the large dimensions lead to a multimode structure. Once the simulation yielded satisfactory results, the waveguide pattern was transferred to our laser-writing machine for direct generation of the mask pattern.

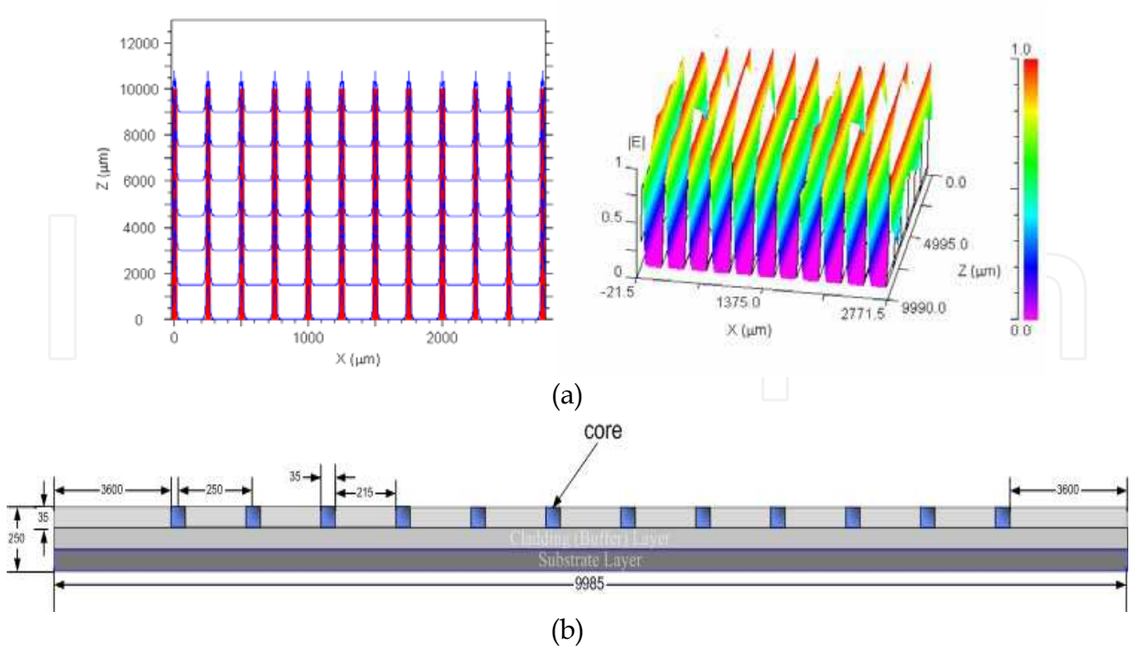

Fig. 6. a) 12 channel waveguide array designed using BeamProp software, and b) cross section schematic and dimensions of the waveguide array.

After generating the mask model, a silicon wafer with various waveguide array patterns was fabricated using conventional photolithographic techniques. Soft lithography was then employed to produce a high-resolution mold of the master pattern. A picture of the transparent mold generated is presented in Fig. 7a. Following mold generation, several channel waveguide array patterns were produced on a silicon substrate wafer, as shown in Fig. 7b. In addition, a micrograph of the 35 μm wide waveguide array is depicted in Fig. 7c.

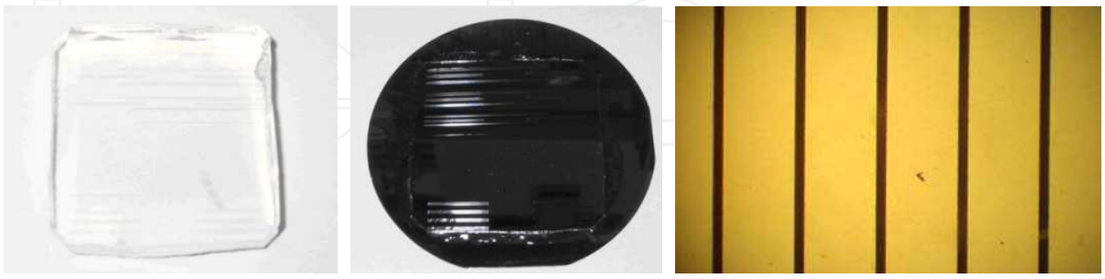

(a) (b) (c)

Fig. 7. a) Soft lithographic mold of waveguide array master pattern and b) subsequent waveguide arrays fabricated on silicon substrate using soft lithography. c) Micrograph (20x objective) of 35 μm wide waveguide array.

The demonstration of channel waveguide arrays on a silicon substrate led to the investigation of similar waveguide fabrication on flexible substrates. We explored the use of different types of soft polymer substrates where the ideal material should be low cost, robust, impact resistant and durable. In addition, properties of high bending radius, UV curing compatibility, excellent thermal resistance, and optical transparency are desired.
Polymer sheets of PETG Vivak® co-polyester material were chosen for the waveguide device substrate. The Vivak® sheet is a low-cost, transparent, thermoplastic sheet widely used for assorted engineering applications. The co-polyester provides superior impact strength, durability and performed well under high-intensity UV illumination. A picture of the flexible waveguide array fabricated through μTM is shown in Fig. 8a. We observed no thermal shrinkage of the co-polyester sheet during UV illumination and the waveguide cladding and core materials bonded and adhered effortlessly to the flexible substrate. Furthermore, flexible waveguide arrays produced on substrates as thin as 200 μm were successfully demonstrated.

(a) (b)

Fig. 8. a) Flexible ribbon array waveguide on co-polyester substrate and b) resulting output mode spots emerging from waveguide array device.

Successful fabrication of our AWEC waveguides was followed by waveguide performance testing. Here elementary waveguide coupling into the channel array was examined. Resulting output beam spots emerging directly from the optical waveguide array device are

shown in Fig. 8b. A VCSEL array source (850 nm wavelength) was used to simultaneously incite all of the array waveguides and light confinement in all channels was achieved. Mode profile non-uniformity can be attributed in part to the lack of optical preparation (and polishing) on waveguide edge facets. For improved edge quality and coupling performance advanced polishing machines for polymer substrates or end facet preparation through excimer laser micromachining has been demonstrated (Jiang, et al., 2004).

After stamp production, the rest of the processes are straightforward replication steps, appropriate for mass production, similar to the stamping of a compact or digital videodisk. While soft lithographic fabrication techniques provide a low-cost, mass production solution, our microtransfer molding approach has some drawbacks. Namely, in μTM the PDMS replica stamp is forcibly pressed against the device substrate, which leads to the creation of a small planar waveguide layer underneath the channel core. Such undesirable byproduct may hinder waveguide alignment, coupling efficiency and propagation loss performance. In the ensuing section we introduce a novel soft lithographic fabrication technique that eliminates the required pressing action and waveguide residue layer through a vacuum assisted microfluidic approach.

4. Vacuum assisted microfluidic waveguide fabrication

Currently, microfluidic guided wave devices based on liquid core waveguide structures are being investigated. Microfluidic optical waveguides have been constructed by inserting liquid into a rectangular channel, where light is guided when the index of the liquid exceeds the surrounding medium (Mach et al., 2002). As another example, liquid-core/liquid-cladding (L^2) optical waveguides have been demonstrated where an optically dense fluid flows in a microfluidic channel within an envelope of fluid with lower refractive index (Wolfe et al, 2004). While these optofluidic waveguides work well in certain biological or analytical instrumentations, their liquid state hinders their applicability in rugged optical communication and photonic applications. Hence, a majority of photonic components manufactured via soft-lithography have been developed through μTM or μCP techniques.

In the preceding section, we employed a μTM scheme to develop guided wave devices where multimode channel waveguide arrays were configured. Such fabrication, where an external force is applied to create the replicated device inevitably leads to the formation of polymer background residue; an unavoidable trait in contact based soft lithography. As the stamp is depressed, the solution on the substrate is forced into the waveguide structure and the excess solution escapes to the edges of the mold. The solution that does not escape forms pockets surrounding the waveguides, resulting in the creation of a planar film layer along the channel waveguide after curing.

When the layer is thick enough, it can become an undesirable planar waveguide, greatly affecting the overall waveguide performance or inducing channel-to-channel crosstalk. Even when the layer is thin, it can still affect the channel waveguide confinement resulting in unfavorable waveguide mode profile changes and modal effective index changes. The strong physical contact on the mold can also lead to pattern deformation and warped structures. Hence, the background polymer residue can alter the desired optical performance of the guided wave device.

Several possible solutions have been addressed to eliminate polymer background residue, including decreasing the applied force. Nonetheless, it was shown that the force with which the mold is depressed has little effect on the polymer background residue (Paloczi, et al.,

2004). In addition, post processing chemical or plasma etching for reducing the residue not only increases manufacturing costs but may affect overall device features such as smoothness and reduction of waveguide thickness. Recently, a new approach for residue reduction was proposed by altering the concentration of the polymer solution (Paloczi, et al., 2004). Since the residue thickness is dependent on the solution viscosity and density, the background residue can be marginally reduced. However, by thinning the solution, it may reduce the waveguide refractive index resulting in poor waveguide confinement and other device performance including electro-optic effects. In addition, the thickness of the waveguides is subsequently reduced because there is not enough solid density in the volume of the solution.

Towards that end, a vacuum assisted microfluidic (VAM) technique was developed that can circumvent such drawbacks. Although based on microfluid filling of the channel device, the microfluidic resin is cured for the creation of solid core structures. The master and PDMS stamp are produced in the same fashion as depicted in Fig. 2. The UV curable core and cladding resins remain the same as well. However, before mold replication, posts are placed on the master to generate holes for the microfluidic inlet reservoir and outlet suction, respectively. To further illustrate the concept, a schematic top view of the proposed VAM technique is presented in Fig. 9.

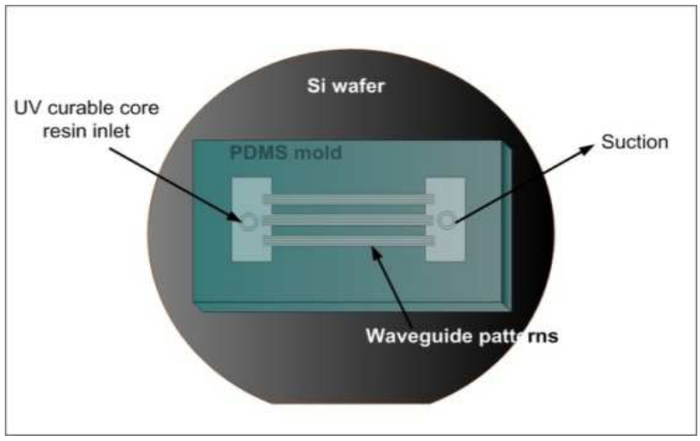

Fig. 9. Schematic of vacuum assisted microfluidic approach for waveguide fabrication.

The process design flow is depicted in Fig. 10. A UV curable cladding layer is spin coated and cured upon the desired substrate as seen in Fig. 10a. Then, the PDMS mold and substrate material are placed in conformal contact and a drop of UV curable core resin is placed through the inlet (see Fig. 10b). Next, rapid filling of the microfluidic channels is assisted by an aspirator (vacuum of 20 mbar) or syringe attached to the outlet opening. The moderate suction provided by an aspirator avoids bubble creation or channel deformation that can be normally caused by strong suction devices such as a rotary or diffusion vacuum pumps. Once filled, the mold is exposed to UV irradiation (20,000 mW/cm^2) and cured for 30 seconds as shown in Fig. 10c. After curing the mold is peeled off to reveal the replicated guided wave structure (Fig. 10d). Lastly, an upper cladding layer may be added, as shown in Fig. 10e. A top view picture of the PDMS microchannel structure along with the inlet and outlet orifices of the stamp is presented in Fig. 10f. Significantly, the quick filling time (1~2 min for 35 μm ×35 μm structure) and fast curing time (30 sec) leads to the rapid prototyping of optical waveguides.

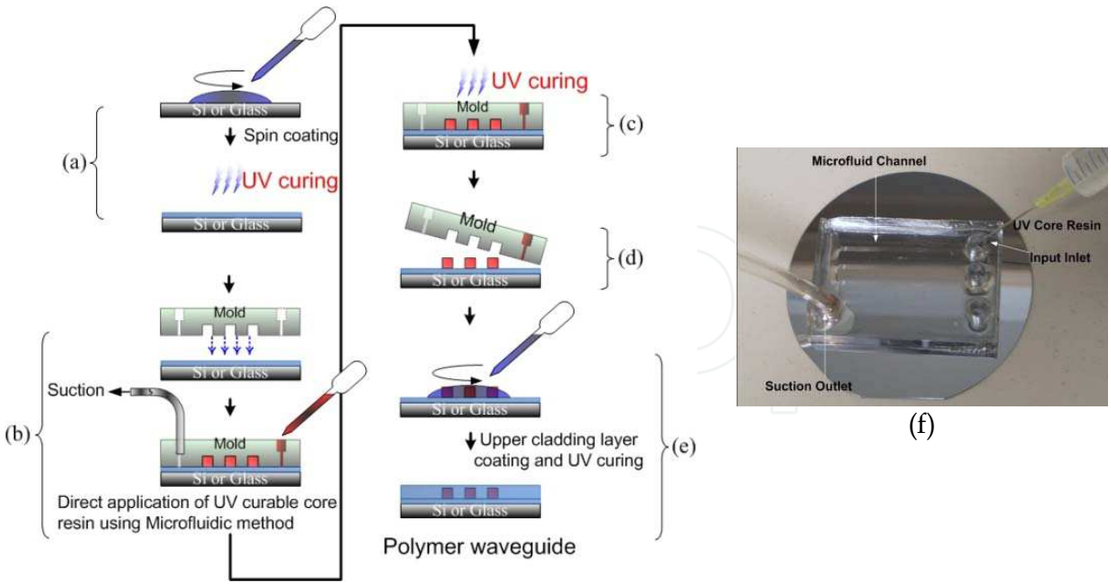

Fig. 10. Process design flow for device replication via VAM. a) UV curable cladding layer is spin coated upon desired substrate. b) After placing PDMS stamp over substrate UV curable core resin drops are placed through an inlet hole. c) Once channels are filled the resin is cured through UV irradiation. d) Stamp is peeled off to reveal the replicated master pattern. e) Upper cladding is coated and cured if desired. f) A top view of the PDMS microchannel structure along with the inlet and outlet orifices of the stamp.

In addition, the VAM method may also be applied to flexible substrates as thin as 200 μm. The ability to fabricate waveguides on rigid substrates (ie., glass, Si) and lithe polymer substrates (co-polyester, polycarbonate, and acrylic) alike, establish the versatility of the VAM approach for fabrication of a wide variety of guided wave devices.

Cross sections of identical waveguides fabricated via both μTM and the VAM technique are detailed in Fig. 11 The sample prepared through μTM contains a thin remnant layer (almost 3~5 microns) due to background residue along the channel structure. In contrast the waveguide prepared through the VAM approach was free of polymer background residue. We also note the improved channel waveguide structure and sidewall edge due to the absence of applied force during the microfluidic fabrication. To further compare both soft lithographic techniques, output mode profile spots of waveguides fabricated by both methods are depicted in the insets of Fig. 11. Once again, improved waveguide formation and elimination of background residue is evident. As a result, a superior mode profile spot is observed via the VAM approach. The images further attest to the elimination of the planar residue layer and satisfactory guided wave channel structure. We cite that the fabrication of the PDMS stamp, core and cladding resins, and UV curing procedures are identical to those previously employed in the μTM approach. Hence, the same low-cost, rapid prototyping of μTM were achieved by VAM while eliminating the cumbersome background residue.

Optical propagation loss is a vital parameter in communication system design. As such, the optical loss performance of the fabricated waveguide arrays was analyzed via the cutback method. As expected, improved waveguide formation through use of the microfluidic technique resulted in lower optical loss. The μTM waveguides exhibited an average loss of 1.1 dB/cm, while the microfluidic waveguide approach generated a loss of 0.68 dB/cm

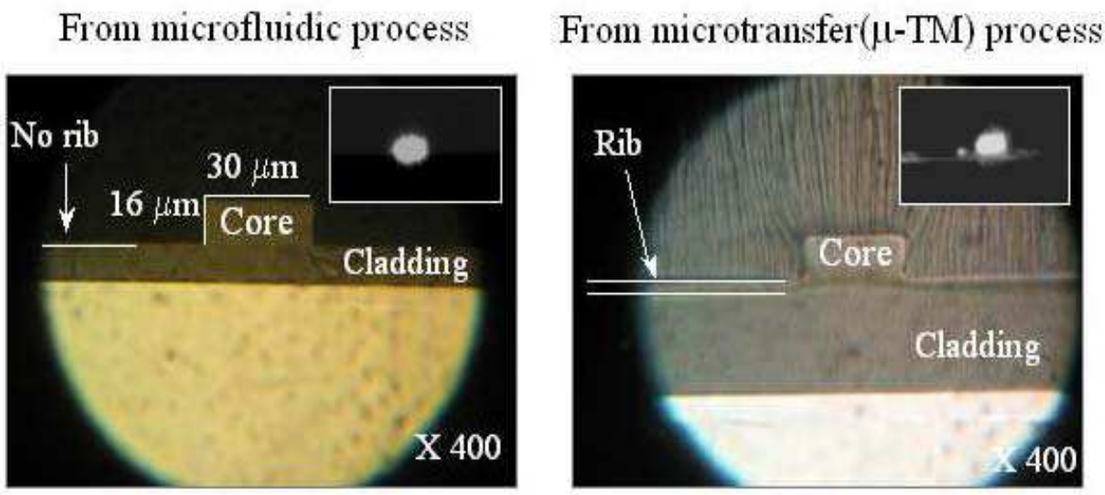

Fig. 11. Waveguide cross-section comparisons of μTM waveguide (right) and VAM waveguide (left). Image confirms elimination of polymer background residue and superior device formation through VAM.

using identical UV curable resins. A plot of the average transmitted power versus waveguide lengths for both methods is presented in Fig. 12 (measurement wavelength of 660 nm). The waveguide losses are attributed in part to the unpolished facet edges and optical preparation of the input and output facets should yield much improved loss performance. Nevertheless, propagation loss reduction (nearly half) is clearly demonstrated, most probably due to the improved waveguide core and reduced defect scattering. Likewise, the reduced waveguide losses further validate the VAM approach for inexpensive, mass fabrication of guided wave devices.

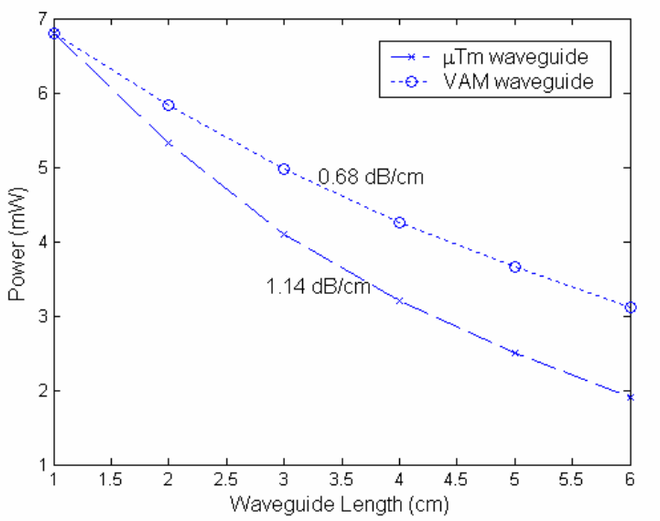

Fig. 12. Average transmitted power versus waveguide length for both μTM and VAM methods.

A lower cost, rapid prototyping, and high resolution patterning soft lithographic technique has been formulated. Furthermore, low-cost polymer materials exhibiting excellent

broadband optical transparency, tunable index control, rapid curing, and light guiding functionality were developed in accordance with the fabrication method. More importantly through the VAM approach, microscopic and SEM analysis depicts improved waveguide structures with no bubbles, defects or planar rib layers. The VAM approach also results in lower propagation losses due to the improved sidewall edges and polymer background residue elimination.

5. VAM fabrication of guided wave devices

In this section we detail the fabrication of several integrated optic and guided wave devices. The VAM technique is used to develop single and multi-mode channel waveguides and array waveguide evanescent coupler (AWEC) ribbons for high-speed optical interconnection (Flores, et al., 2008). The fabrication of these devices demonstrates the cost effectiveness and promise of the proposed approach for the development of inexpensive, mass fabrication of polymer guided wave devices.

5.1 Single mode waveguide

Waveguides can be classified according to the total number of guided modes within the steering structure. Guided wave structures designed to carry only a single allowed propagation parameter are termed single-mode waveguides. Correspondingly, multimode waveguides are designed to accept multiple modes within a guided wave device. The light propagating in each mode has a distinct angle of incidence θ_m (m = 1, 2, 3…), and travels in the z direction with a phase velocity and propagation constant that is characteristic of that mode. In general, guided wave devices designed for long distance applications (> km) employ single-mode structures, while less-expensive and more efficient multimode configurations are used for communication over shorter distances (< km).

In the section 3.1, multimode waveguide arrays were devised through a μTM technique. Multimode guided wave devices offering excellent propagation path stability and lower production costs appear to have excellent potential for card-to-backplane optical interconnect applications. Specifically, the development of multimode guides for high speed optical interconnects will be discussed in a later section. Likewise, single mode waveguides guiding only the fundamental mode have a variety of applications for long distance telecommunications. Particularly, multimode waveguides supporting up to thousands of modes can lead to undesirable modal dispersion effects which are avoided in single mode structures.

Single mode waveguides were developed in accordance with the μTM and VAM techniques. The resins used for the cladding and core were Epotek OG 169 and Norland Optical Adhesive (NOA) 74, respectively. Epotek OG 169 and NOA 74 have viscosities of 200 and 80 cps, respectively and cured refractive indices of 1.5084 and 1.51 for the 1550 nm wavelength, respectively. In particular NOA 74 was chosen for its relatively low viscosity and its higher refractive index relative to the cladding. The low refractive index difference of 0.0016 yields a numerical aperture (NA) of 0.07. Subsequently, a channel waveguide with dimensions of 5 μm x 9 μm was devised to demonstrate single mode performance.

Referring to the channel waveguide dimensions and numerical aperture the number of modes in a channel structure can be approximated as (Saleh, B. & Teich, M., 1991)

$$M = \frac{\pi}{4}\left(\frac{2}{\lambda}\right)^2 d_x d_y NA_x NA_y \,, \tag{1}$$

where d_x and d_y represent the horizontal and vertical geometrical dimensions and NA the numerical aperture ($\left(n_{core}^2 - n_{clad}^2\right)^{1/2}$). Hence, the 5 μm × 9 μm rectangular waveguide (M<1) is single mode at the 1550 nm wavelength. A mode profile of the single mode waveguide fabricated through the VAM method is shown in Fig. 13a. For comparison, the multimode (35 μm x 35 μm) profile spot at the same wavelength is depicted in Fig. 13b. Significantly, both single and multimode waveguides with excellent structural quality were created through the VAM technique. Fig. 13c shows the mode field distribution of the single mode waveguide captured by a beam profiler. The Gaussian intensity distribution and subsequent single mode field profile is observed. In general, although single mode waveguides outperform their multimode counterparts they are deemed too costly and impractical for short distance applications. Through both the μTM and VAM methods, the low cost outlays for both single mode and multimode waveguides are identical. Notably, low cost and rapid prototyping production of single mode waveguides with tight fabrication and alignment tolerances has been accomplished.

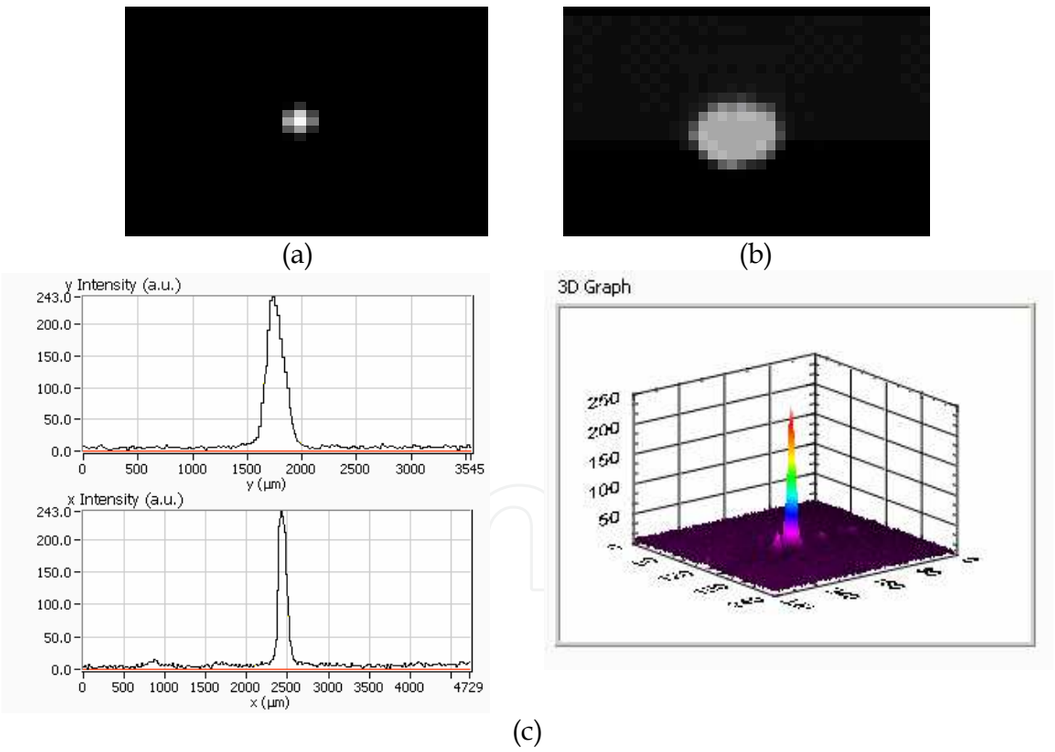

Fig. 13. Channel waveguide mode spots of a) single mode and b) multimode waveguides fabricated via VAM. c) Single mode VAM waveguide beam profile showing x and y axis transverse fields and 3D intensity plot.

An important consideration when using VAM is that unlike μTM (in general), the viscosity of the core resins plays a significant role in the realization of channel waveguide structures.

Low viscosity core resins allow for improved laminar flow, which in turn allows for a quicker distribution among the channels. The tradeoff though comes at the potential cost of intermittent formation of bubbles and a non-uniform density profile along both the length and the central axis (i.e. a dense central region relative to the sides) of the waveguide. On the other hand, high viscosity core resins do not have these associated problems (or at least not as prevalent), but must contend with a slower filling rate and the increased occurrence of partially complete channels. For our fabricated waveguides, low viscosity resins were used for the core material to achieve complete filling of the waveguide channels as the use of higher viscosity resins, especially those with viscosities over 500 cps, often resulted in partial, and/or sparsely filled channels. In particular, as the cross sectional feature size, through which the fluid propagates, is reduced, lower viscosity resins are necessary for successfully filling the channels. Specifically, formation of the smaller dimension single mode waveguides was only accomplished with low viscosity resins (under 200 cps).
Comparison of the cross sections of the single mode channel waveguides fabricated by both the μTM and VAM techniques, are shown in Fig. 14. Similar to the multimode waveguides, shown in Fig. 11, the sample prepared through μTM contains a thin remnant layer (~3 microns) due to background residue along the channel structure. In contrast the waveguide prepared through the microfluidic approach was free of polymer background residue. Once again, improved waveguide formation and elimination of background residue by VAM is evident.

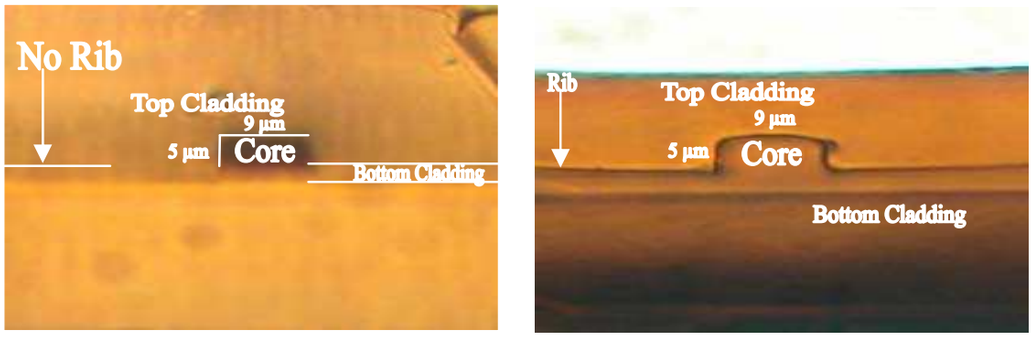

Fig. 14. Waveguide cross-section comparisons single mode waveguides fabricated by VAM technique and by μTM technique. Image reaffirms the elimination of polymer background residue and superior device formation through VAM.

5.2 Array waveguide evanescent coupler ribbon

Recent advances in computing technology have highlighted deficiencies with electrical interconnections at the motherboard and card-to-backplane levels. Specifically, the CPU speeds of computing systems are drastically increasing with on-chip local clock speeds expected to approach 6 GHz by 2010 (International SEMATECH, 2007), yet, card-to-backplane communication speed is unable to maintain the same pace. Due to severe frequency dependant physical factors such as crosstalk, power dissipation, packaging density, and electromagnetic interference (EMI); copper interconnections used on existing motherboards are expected to cause drastic bottleneck problems for board-to-board or off-chip data bus transfers.
Consequently, optical links have been extensively researched for high-speed backplane applications (Glebov, et al., 2005). The most significant benefit that optical interconnects

provide over electrical links is the tremendous gain in bandwidth capacity. For example, the bandwidth capacity of a single optical interconnect (guided wave) line was experimentally characterized to be 2.5 THz (Kim, G. & Chen, R. T., 1998), and the bandwidth capacity of optical silica fibers can theoretically reach speeds of up to 50 THz (Kogelnik, 2000). In addition, attenuation losses in optical interconnects are data rate and EMI independent, and offer improved packaging densities. Actively researched solutions at the board-to-board level include free-space optical interconnects, guided-wave interconnects, and fiber based links. While each approach appears promising for future card-to-backplane applications various drawbacks must be addressed before optical links replace copper interconnections inside computers.

For example, the guided-wave approach offers excellent interconnect path stability, low cost processing (ie., polymer waveguides) and are suitable for multi-drop interconnect architectures. However, a major obstacle in guided-wave techniques is the need of 90° out of plane optical deflectors to couple light into or out of the interconnecting waveguides (Glebov, et al., 2007). Such micro-mirrors suffer from reflection losses (i.e., 0.5 dB) due to roughness of diced surface and absorption and scattering of the metal film. Additional microlenses or fiber-coupler adaptors are also regularly used to assist the out-of-plane deflector. These constraints increase manufacturing complexity and cost, degrades backplane reliability, and results in local waveguide terminations (deflecting mirror reflects all light preventing further waveguide transmission for multi-drop interconnects).

Moreover, the out of plane deflectors are not energy efficient since they consume optical power even when cards are not plugged into the backplane. Previously, we reported on the concept of array waveguide evanescent couplers (AWEC) for card-to-backplane optical interconnections (Yang, et al., 2007). By evanescently tapping optical signal power from a backplane bus to a flexible optical bus on the daughter card, the proposed concept eliminates local waveguide termination and the use of 45° micro-mirrors or prisms for the 90° out of plane turns. An initial AWEC optical ribbon link was successfully demonstrated. Nevertheless, the initial AWEC ribbons were limited by excessive manufacturing and fabrication costs (photolithography) and the reported operating speed was limited to 2.5 GHz.

As a result, a VAM approach is adopted for AWEC fabrication. The high-resolution rapid AWEC prototyping technique can result in overall lower coupler fabrication and system cost. A schematic of the proposed AWEC technique and its use for multicard backplane optical interconnects is shown in Fig. 15. The interconnection scheme is based on the exposed core evanescent coupling between a backplane waveguide bus and a flexible bus connected to the plug-in card (or daughter board). Comparable to electronic backplanes, a plug-in card can simply be plugged into the designated backplane AWEC connector to gain access to shared media bus.

Our AWEC interconnect technique is able to efficiently tap optical signal power from the backplane waveguide to card waveguide without any local waveguide terminations. The diagram demonstrates high-speed signals exiting the backplane waveguide without the use of 45° micro-mirrors or prisms. In this particular case, the backplane waveguide signal is evanescently routed to an identical waveguide in the plug-in card, through a flexible AWEC ribbon. A locking mechanism is used to control the interaction length and allow a relatively uniform pressure for consistent power coupling from the backplane waveguide to the AWEC card ribbon. The locking device can be made automatic using spring loaded mechanism not presented herein.

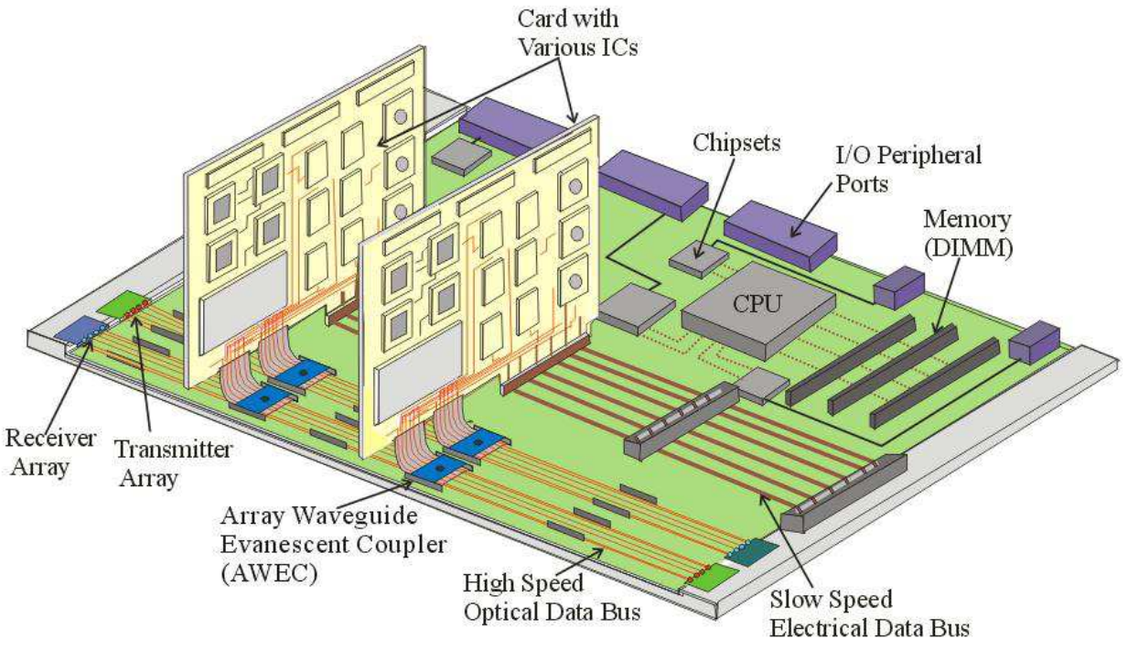

Fig. 15. Schematic detailing AWEC optical interconnect technique for card-to-backplane motherboard applications.

The operational principle of the AWEC technique can be explained by the directional coupling (Yariv, 1973) between the waveguide on the AWEC ribbon and its counterpart on the backplane surface. We consider a general AWEC waveguide structure with a refractive index distribution given by

$$n^2(x,y) = \begin{cases} 1, & |y| < d, \quad all\ x \\ n_{core}, & d \le |y| \le 2a + d, \quad |x| \le a \\ n_{clad}, & 2a + d < |y| \le 2a + 2b + d, |x| \le c \end{cases}, \tag{2}$$

where all dimensions are defined in Fig. 16 except that the coordinate origin is at the center of the waveguide gap. Two waveguides, labeled W_1 and W_2, which are initially separated, are brought close to one another over some interaction length L. When the two waveguides are closely spaced and aligned in the lateral direction, the evanescent fields of the guided modes in the two waveguides overlap causing an alteration of the optical mode and field distributions of the waveguide system.

Due to the weakly guided nature of the AWEC system (Δn = 0.011), coupled mode analysis (Yariv, 1973) can be used to analyze the electromagnetic behavior of the complete structure. In this regard, the goal of the coupled-mode theory is to express the electromagnetic fields of the complete structure as a superposition of the unperturbed waveguide electric fields. Most importantly, the coupled-mode theory assumes that the waveguide modes remain approximately the same and the coupling interaction modifies the amplitudes of the modes without affecting the modal transverse field distributions or propagation constants of the waveguides. Thus, in the presence of waveguide coupling the modal amplitudes in the two waveguides become functions of the propagation path z.

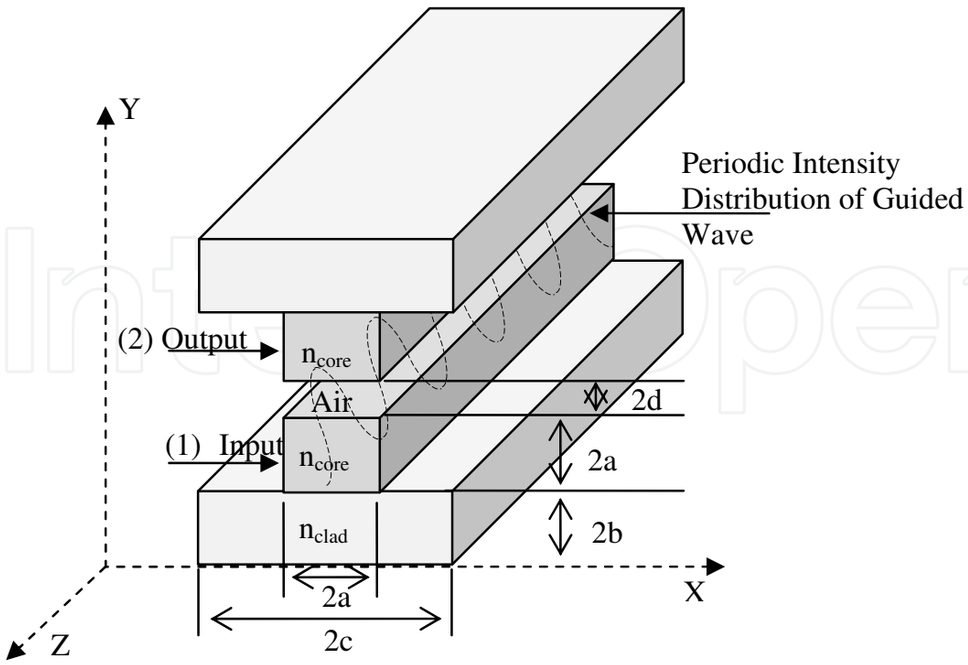

Fig. 16. Diagram depicting AWEC coupling structure and directional coupling between two parallel channel waveguides.

The overlapping fields result in the modification of the waveguide mode solutions and the introduction of an energy exchange coupling constant between the two waveguide modes. Through the coupled-mode theory, the optical powers of the propagating modes in the two channel waveguides, $P_1(z)$ and $P_2(z)$, can be approximated as

$$P_1(z) = P_1(0)\cos^2 \kappa z$$

$$P_2(z) = P_2(0)\sin^2 \kappa z, \tag{3}$$

when the two waveguide channels are phase matched. Here, κ is the propagation constant of the waveguide mode. $P_1(0)$ and $P_2(0)$ are the initial light power of the two waveguide channels, respectively.

Notably, the coupling constant κ is proportional to channel separation. Although the coupling coefficient can be controlled through pressure regulation between the two waveguides, - which in turn influences waveguide separation - precise pressure control is both impractical and difficult to achieve. For the AWEC case, the waveguide interaction length will be employed to deliver the desired coupling coefficient, as the variation of the interaction length on the millimeter scale is much easier to resolve and repeat. By adjusting the interaction length between waveguides, the amount of energy transferred and coupling efficiency between the guides can be regulated.

It is important to mention that the coupled-mode analysis discussed above pertains to single-mode channel waveguides. The more pertinent case of multimode waveguides can be analyzed by noting that the complex optical fields are a superposition of all the modes

excited within the channel. As such CAD simulations modeled via BeamPROP were executed to examine multimode coupler behavior between the AWEC ribbons (Flores, et al, 2008). CAD simulation results demonstrated strong evanescent coupling between the AWEC ribbons and dominant energy distribution (> 90%) within the fundamental mode and agreed well with the experimental coupling results.

To demonstrate effective AWEC coupling, flexible ribbon arrays identical to the multimode arrays presented in Fig. 6 were fabricated via a VAM approach. The flexible ribbon arrays consist of 12 channels with a 250 μm pitch for integration into commercial parallel optical transmitter/receiver array modules. By incorporating a soft lithographic method we were able to generate the waveguide arrays essential for AWEC fabrication without the intricate use of conventional photolithography. Moreover, a scanning electron micrograph (SEM) of a multi-channel AWEC device fabricated on a silicon substrate is shown in Fig. 17. The image once again attests to the elimination of the planar rib layer and satisfactory guided wave channel structure.

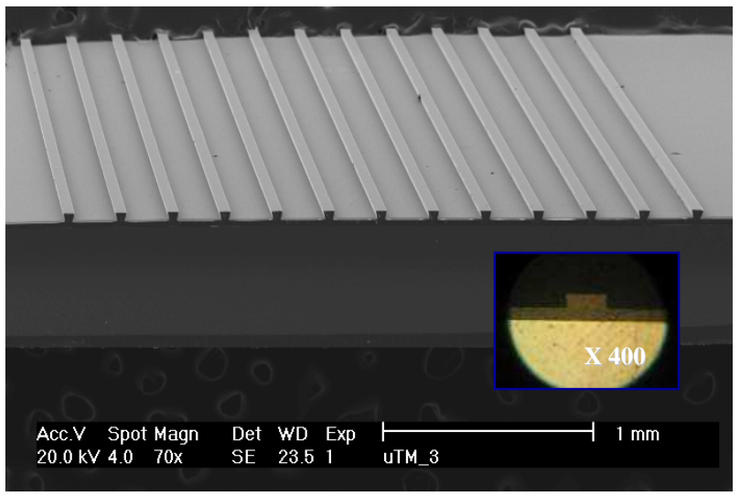

Fig. 17. SEM photograph of the replicated AWEC device fabricated via soft lithography. Inset shows a cross-section micrograph of an AWEC channel.

For the optical interconnection, the flexible waveguide ribbons were integrated into parallel optical transmitter array and receiver array modules. One flexible ribbon was interfaced to the VCSEL transmitter board, while another ribbon was connected to the PIN receiver board and the two AWEC ribbons displaced at 90° were then evanescently coupled at an interaction length of 11 mm. Index matching fluid (n = 1.515) was inserted between the ribbons to facilitate coupling as predicted by the simulation results. Successfully, at speeds of up 10 GHz we were able to easily demonstrate evanescent coupling of pulse data information. We note that our high speed link was solely limited by our electronic signal generator and digitizing oscilloscope which cannot operate beyond 10 GHz.

Figure 18 shows the 10 Gbps eye diagram for the AWEC optical interconnect link. Optical interconnections at 10 Gbps have been successfully achieved for each of the 12 channels on the AWEC ribbon, resulting in an aggregate data rate of over 100 Gbps. The modal dispersion analysis for the multimode waveguide predicts speeds of up to 40 Gbps can be accommodated for each interconnect channel (Flores, et al., 2008).

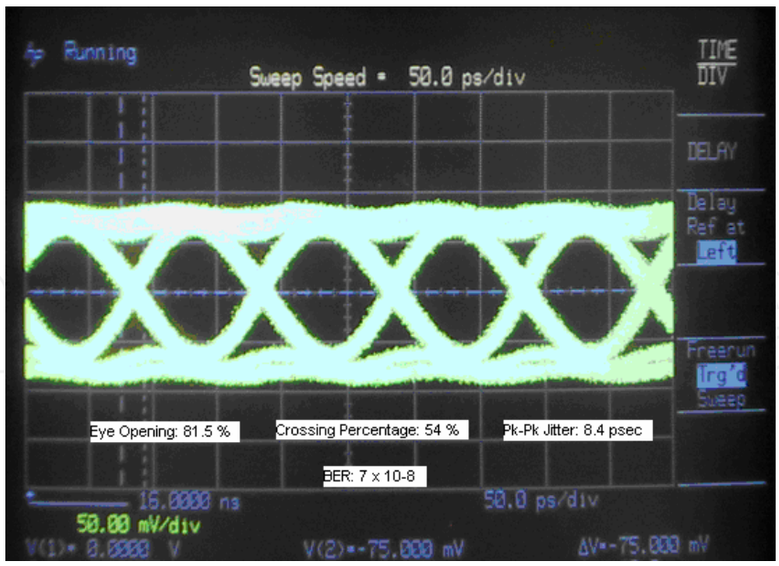

Fig. 18. Recovered eye diagram for our AWEC link at 10 Gbps.

6. Conclusions

The design and development of guided wave devices based on soft lithographic fabrication techniques was examined. Notably, a novel vacuum assisted microfluidic technique for fabrication of guided wave and integrated optical devices was described. Importantly, the technique eliminates the polymer background residue inherent to traditional soft molding fabrication techniques. In addition, UV curable resins with tunable index control specifically tailored for soft lithography were developed.

Comparisons to conventional soft lithography demonstrate that the VAM approach results in lower propagation losses, lower crosstalk, and improved waveguide structures. More importantly, microscope analysis portrays improved device formation, sidewall edges and the elimination of the polymer background residue intrinsic to conventional soft lithography. As a low-cost rapid prototyping technique the VAM soft lithographic method allows guided wave devices to be implemented rapidly and inexpensively.

Moreover, through adoption of our VAM technique we were able to successfully fabricate several integrated optic and guided wave devices. The VAM technique is used to develop single and multi-mode channel waveguides, and array waveguide evanescent coupler (AWEC) ribbons for high-speed optical interconnection. Notably, through a soft lithographic approach the overall fabrication costs were reduced (without sacrificing ribbon quality and performance) and data rates of up to 10 Gbps per channel were demonstrated. We expect that the AWEC scheme will be significant for high-speed optical interconnects in advanced computing and backplane systems. Overall, we believe that the novel VAM technique can yield lower production costs and manufacturing complexity for polymer based photonic integrated circuits.

7. Acknowledgements

The projects were supported in part by the Department of Defense and the American Society for Engineering Education.

8. References

Bowers, J. E.; Park, H; Kuo, Y. –H; Fang, A. W.; Jones, R.; Paniccia, M. J.; Cohen, O. & Raday, O. (2007). Integrated Optical Amplifiers on Silicon Waveguides. *Integrated Photonics and NanoPhotonics Research and Applications (IPNRA)* 2007, ITuG1.

Brown, T. G.; Bradfield P. L.; Hall D. G. & Soref R. A. (1987). Optical emission from impurities within an epitaxial-silicon optical waveguide. *Optics Letters*, Vol. 12, No. 9, 753-755.

Flores, A.; Song, S.; Yang, J. J.; Liu, Z. & Wang, M. R. (2008). High-speed optical interconnect coupler based on soft lithography ribbons. *IEEE Journal of Lightwave Technology*, Vol. 26, No. 13, 1956-1963.

Glebov, A. L.; Roman, J.; Lee, M. G. & Yokouchi, K. (2005). Optical interconnect modules with fully integrated reflector mirrors. *IEEE Photonic Technology Letters*, Vol. 17, No. 7, 1540-1542.

Glebov, A. L.; Lee, M. G. & Yokouchi, K. (2007). Integration technologies for pluggable backplane optical interconnect systems. *Optical Engineering*, Vol. 46, No. 1, 015403-015410.

Grundy, K.; Liaw, H.; Otonari, G. & Resso, M. (2006). Designing scalable 10G backplane interconnect systems utilizing advanced verification methodologies. *DesignCon 2006*, Paper 8-WP2.

Heckele, M. & Schomburg, W. K. (2004). Review on micromolding of thermoplastic polymers. *Journal of Micromechanics And Microengineering*, Vol. 14, No. 3, R1-R14.

Heinrich, J.; Zeeb, E. & Ebeling, K. J. (1997). Butt-coupling efficiency of VCSELs into multimode fibers. *IEEE Photonics Technology Letters*, Vol. 9, No. 12, 1555-1557.

International SEMATECH (2007). The National Technology Roadmap for Semiconductors (ITRS)- Technology. Semiconductor Industry Association.

Jiang, J.; Callender, C. L.; Noad, J. P.; Walker, R. B.; Mihailov, S. J.; Ding, J. & Day. M (2004). All-polymer photonic devices using excimer laser micromachining. *IEEE Photonics Technology Letters*, Vol. 16, No. 2, 509-511.

Kim, G. & Chen, R. T. (1998). Three-dimensionally interconnected bidirectional optical backplane. *IEEE Photonic Technology Letters*. Vol. 11, No. 7, 880-882.

Kogelnik, H. (2000). High-capacity optical communication. *IEEE Journal of Selected Topics in Quantum Electronics*. Vol. 6, No. 6, 1279-1286.

Kunnavakkam, M. V.; Houlihan, F. M.; Schlax, M.; Liddle, J. A.; Kolodner, P.; Nalamasu, O. & Rogers, J. A. (2003). Low-cost, low-loss microlens arrays fabricated by soft-lithography replication process. *Applied Physics Letters*, Vol. 82, No. 8, 1152-1154.

Lauks, I. R. (1998). Microfabricated biosensors and microanalytical systems for blood analysis. *Accounts of Chemical Research*, Vol. 31, No. 5, 317-324.

Liu, S.; Shi, Y.; Ja, W. W.; & Mathies, R. (1999). Optimization of high-speed DNA sequencing on microfabricated capillary electrophoresis channels. *Analytical Chemistry*, Vol. 71, No. 3, 566-573.

Mach, P.; Dolinski, M.; Baldwin, K. W.; Rogers, J. A.; Kerbage, C.; Windeler, R. S. & Eggleton, B. J. (2002). Tunable microfluidic optical fiber. *Applied Physics Letters*, Vol. 80, No. 9, 4294-4296.

Paloczi, G. T.; Huang, Y.Y.; Scheuer, J. & Yariv, A. (2004). Soft lithography molding of polymer integrated optical devices: reduction of background residue. *Journal of Vacuum Science and Technology B*, Vol. 22, No. 4, 1764-1769.

Ramaswamy R. V. & Srivastava R. (1988). Ion-exchanged glass waveguides: a review. *IEEE Journal of Lightwave Technology*, Vol. 6, No. 6, 984-1000.

Rogers, J. A.; Meier, M. & Dodabalapur, A. (1998). Using printing and molding techniques to produce distributed feedback and Bragg reflector resonators for plastic lasers. *Applied Physics Letters*, Vol. 73, No. 13, 1766-1768.

Saleh, B. E. & Teich, M. C. (1991). *Fundamentals of Photonics*. John Wiley & Sons, ISBN: 0471839655, New York.

Saleh, O. A. & Sohn, L. L. (2003). An artificial nanopore for molecular sensing. *Nano Letters*, Vol. 3, No. 1, 37-38.

Santini, J.T.; Cima, M. J. & Langer, R. (1998). A controlled-release microchip. Nature, Vol. 397, No. 6717, 335-338.

Schueller, O. J.; Whitesides, G.; Rogers, J. A.; Meier, M. & Dodabalapur, A. (1999). Fabrication of photonic crystal lasers by nanomolding solgel glasses. *Applied Optics*, Vol. 38, No. 27, 5799-5802.

Song, S.; Flores, A.; Yang, J. J. & Wang, M. R. (2005). Fabrication of multimode polymer waveguide by using soft lithographic technique. *OSA Annual Meeting 2005*, Tuscon, Az., FThQ7.

Quist, A. P.; Pavlovic, E. & Oscarsson, S. (2005). Recent Advances in microcontact printing: Analysis of biomaterials. *Analytical and bioanalytical chemistry*, Vol. 381, No. 3, 591-600.

van der Berg, A.; Grisel, A.; Verney-Norberg, E.; van der Schoot, B. H.; Koudellka-Her, M. & de Rooij, N. F. (1993). On-wafer fabricated free-chlorine sensor with ppb detection limit for drinking-water monitoring. *Sensors and Actuators B*, Vol. 13, No. 1-3, 396-399.

Wang, M. R. & Su, H. (1998). Laser direct-write gray-level mask and one-step etching for diffractive microlens fabrication. *Applied Optics*, Vol. 37, No. 32, 7568-7576.

Whitesides, G. M. (2006). The origins and the futures of microfluidics. *Nature*, Vol. 442, No. 7101, 368-373.

Wolfe, D. B.; Conroy, R. S.; Garstecki, P.; Mayers, B. T.; Fischbach, M. A.; Paul, K. E.; Prentiss, M. & Whitesides, G. M. (2004). Dynamic control of liquid-core/liquid-cladding optical waveguides. *Proceedings of the National Academy of Sciences USA*, Vol. 101, No. 34, 12434-12438.

Xia, Y.; Kim, E.; Zhao, X.; Rogers, J. A.; Prentiss, G. M. Whitesides, G. M. (1997). Complex optical surfaces formed by replica molding against elastomeric masters. *Science*, Vol. 273, No. 5273, 347-349.

Xia Y. & Whitesides, G. M. (1998). Soft lithography. *Angewandte Chemie International Edition*, Vol. 37, No. 5, 570-575.

Yang, J. J.; Flores, A. & Wang, M. R. (2007). Array Waveguide Evanescent Ribbon for Card-to-Backplane Interconnects. *Optics Letters*, Vol. 32, No. 1, 14-16.

Yariv, A. (1973). Coupled-mode theory for guided-wave optics. *IEEE Journal of Quantum Electronics*, Vol. 9, No. 9, 919-933.

Zhang, F.; Nyberg, T. & Inganas, O. (2002). Conducting polymer nanowires and nanodots made with soft lithography. *Nano Letters*. Vol. 2, No. 12, 1373-1377.

Zhao, X.; Xia, Y. & Whitesides, G. M. (1996) Fabrication of three-dimensional micro-structures: Microtransfer molding. *Advanced Materials*, Vol. 8, No. 10, 837-840.

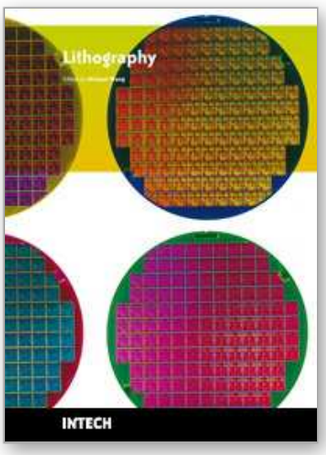

Lithography

Edited by Michael Wang

ISBN 978-953-307-064-3
Hard cover, 656 pages
Publisher InTech
Published online 01, February, 2010
Published in print edition February, 2010

Lithography, the fundamental fabrication process of semiconductor devices, plays a critical role in micro- and nano-fabrications and the revolution in high density integrated circuits. This book is the result of inspirations and contributions from many researchers worldwide. Although the inclusion of the book chapters may not be a complete representation of all lithographic arts, it does represent a good collection of contributions in this field. We hope readers will enjoy reading the book as much as we have enjoyed bringing it together. We would like to thank all contributors and authors of this book.

How to reference

In order to correctly reference this scholarly work, feel free to copy and paste the following:

Angel Flores and Michael R. Wang (2010). Soft Lithographic Fabrication of Micro Optic and Guided Wave Devices, Lithography, Michael Wang (Ed.), ISBN: 978-953-307-064-3, InTech, Available from: http://www.intechopen.com/books/lithography/soft-lithographic-fabrication-of-micro-optic-and-guided-wave-devices

INTECH
open science | open minds

InTech Europe
University Campus STeP Ri
Slavka Krautzeka 83/A
51000 Rijeka, Croatia
Phone: +385 (51) 770 447
Fax: +385 (51) 686 166
www.intechopen.com

InTech China
Unit 405, Office Block, Hotel Equatorial Shanghai
No.65, Yan An Road (West), Shanghai, 200040, China
中国上海市延安西路65号上海国际贵都大饭店办公楼405单元
Phone: +86-21-62489820
Fax: +86-21-62489821

IntechOpen